*Central European Journal of Energetic Materials*, **2013**, *10*(4), 481-493
ISSN 1733-7178

# Preparation, Structure and Kinetic Analysis of the Thermal Behavior of Some Energetic Salts of 3-Hydrazino-4-amino-1,2,4-triazole

Jin-Ting WU, Jian-Guo ZHANG*, Mou SUN, Xin YIN and Tong-Lai ZHANG

*State Key Laboratory of Explosion Science and Technology, Beijing Institute of Technology, Beijing 100081, China*
**E-mail: zjgbit@bit.edu.cn*

**Abstract:** As a key research objective for low melting explosives and propellants, energetic salts have received worldwide attention. 3-Hydrazino-4-amino-1,2,4-triazole (HATr) is an important high-nitrogen compound (73.65% N) with good stability. This paper focuses on the energetic salts which were formed between HATr and picric acid (PA) or 2,4,6-trinitroresorcinol (TNR). Single crystals of HATr·PA and HATr·TNR·$H_2O$ were grown and their crystal structures determined at low temperature. They both belong to the monoclinic system, $P2_1/n$ space group. The thermal characteristics of the two target salts were investigated using DSC and TG-DTG. In addition, the non-isothermal decomposition kinetics, heats of combustion and sensitivity have also been investigated. The detonation pressures (P) and detonation velocities (D) of the salts have been calculated using the K-J equations. The results indicated that both salts have certain potential applications as gunpowder and propellant materials.

**Keywords:** synthesis, crystal structure, thermal analysis, 3-hydrazino-4-amino-1,2,4-triazole, energetic salts

## Introduction

In the search for low melting explosives and propellants, energetic salts have generated widespread interest [1]. Energetic salts are a unique class of highly energetic materials due to their lower vapor pressures and higher densities compared to their atomically similar non-ionic analogs [2]. Their properties can

be carefully tuned via the choice of the component ions, and they are readily optimized and improved through the combination of different cations and anions [3]. Nitrogen-containing heterocycles are one of the sources of energetic salts [4]. Triazole is a high nitrogen-containing ring heterocycle which has a large number N-N and C-N bonds and therefore exhibits a large positive heat of formation [5]. 3-Hydrazino-4-amino-1,2,4-triazole (HATr) is a typical high-nitrogen triazole, with a nitrogen content of 73.65%, and shows good stability.

This paper focuses on the energetic salts which were formed by treating 3-hydrazino-4-amino-1,2,4-triazole (HATr) with picric acid (PA) and 2,4,6-trinitroresorcinol (TNR).

## Experimental Section

***Caution:*** *3-Hydrazino-4-amino-1,2,4-triazole and its salts are energetic materials with increased sensitivities towards shock and friction. Therefore, appropriate safety precautions have to be applied whilst synthesizing and handling them.*

### Materials and physical techniques

All chemical reagents and solvents were analytically pure, commercial products. Elemental analysis was performed with a Flash EA 1112 fully-automatic trace element analyzer. Infrared spectra were measured using a Bruker Equinox 55 spectrometer with KBr pellets. DSC measurements were carried out with a Pyris-1 differential scanning calorimeter at a linear heating rate of 5 $K \cdot min^{-1}$. The energies of combustion were measured using a Parr 6200 oxygen bomb calorimeter.

3-Hydrazino-4-amino-1,2,4-triazole di-hydrochloride [HATr·2HCl] was prepared according to the literature [6]. HATr itself was obtained by reacting 3-hydrazino-4-amino-1,2,4-triazole di-hydrochloride with lithium hydroxide.

### Synthesis of the energetic salts of HATr

*Synthesis of HATr·PA*

A solution of HATr (1.140 g, 10 mmol) in water (50 mL) was added with stirring to a suspension of PA (2.291 g, 10 mmol) in water (50 mL) at 338 K. After stirring for 15 min, the solution was cooled to room temperature. The precipitate was collected by filtration, washed with methanol and dried in air to give the desired product as a yellow solid (2.278 g, 66.4%). IR(KBr): v = 3347, 3256, 3087, 1645, 1559, 1432, 1338, 1159, 1080, 913, 786 $cm^{-1}$; Elemental analysis (%):

found: C 27.94, H 2.65, N 36.76; $C_8H_9N_9O_7$ requires: C 28.00, H 2.64, N 36.73.

*Synthesis of HATr·TNR·$H_2O$*

The same method was used as described for HATr·PA to form the product as a yellow solid (2.268 g, 63.1%). IR(KBr): v = 3348, 3040, 2857, 1993, 1643, 1503, 1311, 1369, 1211, 1053, 912, 858 $cm^{-1}$; Elemental analysis (%): found: C 25.46, H 2.95, N 33.45; $C_8H_{11}N_9O_9$ requires: C 25.47,H 2.94, N 33.42.

**X-ray data collection and structure refinement**

Collection of X-ray data for HATr·PA and HATr·TNR·$H_2O$ was performed on a Rigaku Saturn 724+ CCD diffractometer (Mo $K_\alpha$ radiation, graphite monochromator). The structure was solved using direct methods and successive Fourier difference syntheses (SHELXS-97) [7], and refined using full-matrix least-squares on $F^2$ with anisotropic thermal parameters for all non-hydrogen atoms (SHELXL-97) [8]. Hydrogen atoms were added theoretically and refined with riding model position parameters and fixed isotropic thermal parameters. The basic crystallographic data, measurement and refinement details are summarized in Table 1.

## Results and Discussion

3-Hydrazino-4-amino-1,2,4-triazole hydrochloride was synthesized according to a literature procedure [6] starting from the reaction of the triaminoguanidinium chloride with formic acid, with hydrochloric acid as catalyst under reflux conditions. Lithium hydroxide was then used to neutralize the salt to obtain 3-hydrazino-4-amino-1,2,4-triazole. HATr·PA and HATr·TNR·$H_2O$ were prepared by reacting an HATr aqueous solution with an aqueous suspension of PA or TNR, respectively. Scheme 1 shows the synthesis route for HATr·PA and HATr·TNR·$H_2O$. Both synthetic routes shown are basically acid-base reactions.

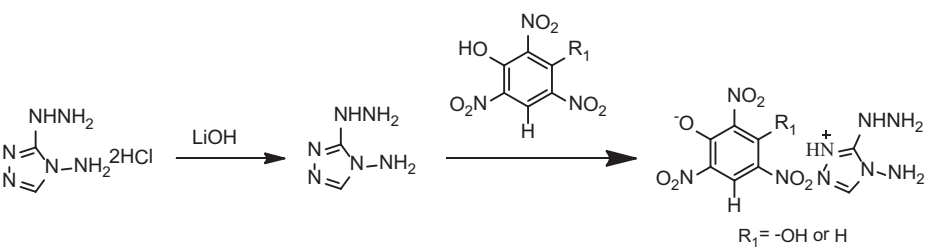


**Scheme 1.** Synthesis routes for 3-hydrazino-4-amino-1,2,4-triazole and its salts.

**X-ray crystallography**

Crystals of HATr·PA and HATr·TNR·$H_2O$ that were suitable for X-ray diffraction were obtained by slow, spontaneous crystallization from water at room temperature. Their structures are shown in Figure 1. Crystallographic and structural refinement data are listed in Table 1, and selected bonds lengths and angles are listed in Table 2.

**Table 1.** X-ray data and parameters

| Items | HATr·PA | HATr·TNR·$H_2O$ |
|---|---|---|
| Empirical formula | $C_8H_9N_9O_7$ | $C_8H_{11}N_9O_9$ |
| Formula mass | 343.24 | 377.26 |
| Temperature (K) | 153(2) | 153(2) |
| Crystal system | monoclinic | monoclinic |
| Space group | $P2_1/n$ | $P2_1/n$ |
| $Z$ | 4 | 4 |
| $a$ (Å) | 6.8928(17) | 15.393(3) |
| $b$ (Å) | 22.670(6) | 5.2670(10) |
| $c$ (Å) | 8.460(2) | 19.042(4) |
| $\beta$ (°) | 96.889(4) | 111.794(3) |
| $V$ (Å$^3$) | 1312.3(6) | 1433.5(5) |
| $D_c$ (g·cm$^{-3}$) | 1.737 | 1.748 |
| $\mu$ ($M_oK_a$) (mm$^{-1}$) | 0.71073 | 0.71073 |
| $F$ (000) | 704 | 776 |
| $\theta$ (°) | 2.586~29.131 | 2.139~29.131 |
| Reflection measured | 13083 | 10308 |
| Independent reflection [$R_{int}$] | 2991 [$R_{int}$=0.0295] | 3796 [$R_{int}$=0.0217] |
| $S$ | 0.998 | 1.002 |
| $R_1$, $wR_2[I>2\sigma(I)]$ | 0.0391, 0.0969 [a] | 0.0384, 0.0967 [b] |
| $R_1$, $wR_2$(all) | 0.0427, 0.1003 [a] | 0.0472, 0.1031 [b] |
| $\Delta\rho_{max}$, $\Delta\rho_{min}$ (e·Å$^{-3}$) | -0.210, 0.043 | -0.284, 0.050 |

[a] $w = 1/[\sigma^2(F_o^2) + (0.0526p)^2 + 0.5800p]$, where $p = (F_o^2 + 2F_c^2)/3$.
[b] $w = 1/[\sigma^2(F_o^2) + (0.0561p)^2 + 0.3600p]$, where $p = (F_o^2 + 2F_c^2)/3$.

Compound HATr·PA: in the PA anion, the C-C bond lengths range from 1.37 to1.45 Å, which is longer than a C=C bond length (1.34 Å) and shorter than a normal C-C bond length (1.54 Å), maintaining the characteristics of a benzene ring. For the triazole ring, the angle of C1-N1-C2 is 106.71(11)°, and the angles of N1-C1-N2 and N1-C2-N3 are 106.15(11)° and 111.92(12)°, respectively. Additionally, the benzene and triazole rings lie in different planes (Figure 2a),

which are inclined at 68.54°.

Compound HATr·TNR·$H_2O$: the structure consists of one HATr cation, one TNR anion and one crystal-water molecule. In contrast to the HATr·PA crystal, the planes of the benzene and triazole rings are almost parallel, with an angle of inclination of 2.2 ° (Figure 2b).

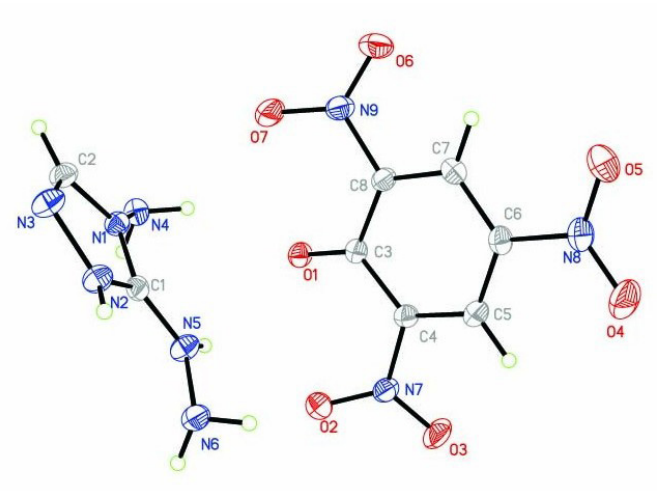


(a)

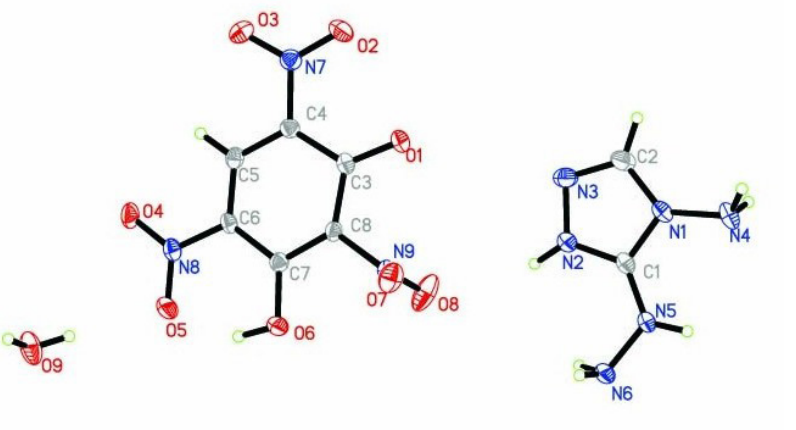


(b)

**Figure 1.** Molecular unit of (a) HATr·PA and (b) HATr·TNR·$H_2O$. Thermal ellipsoids are set to 50% probability.

**Table 2.** Selected bond lengths and angles

| HATr·PA | | HATr·TNR·$H_2O$ | |
|---|---|---|---|
| Bond lengths (Å) | | | |
| O1-C3 | 1.2585(16) | O1-C3 | 1.2525(14) |
| N3-C2 | 1.2924(19) | N1-C2 | 1.3738(18) |
| N5-N6 | 1.4121(17) | N2-N3 | 1.3907(15) |
| N1-N4 | 1.4031(16) | N7-C4 | 1.4465(16) |
| N2-N3 | 1.3927(16) | C3-C4 | 1.4530(17) |
| N9-C8 | 1.4563(17) | N1-N4 | 1.4002(16) |
| Bond angles (°) | | | |
| C1-N1-C2 | 106.71(11) | C1-N1-C2 | 106.89(11) |
| C2-N3-N2 | 104.18(11) | C2-N1-N4 | 131.36(11) |
| N5-C1-N2 | 127.98(13) | O8-N9-C8 | 119.24(10) |
| O3-N7-C4 | 118.28(12) | N5-C1-N1 | 124.49(12) |
| N2-C1-N1 | 106.15(11) | C8-C3-C4 | 112.28(10) |
| O6-N9-C8 | 117.95(12) | O1-C3-C8 | 120.39(11) |

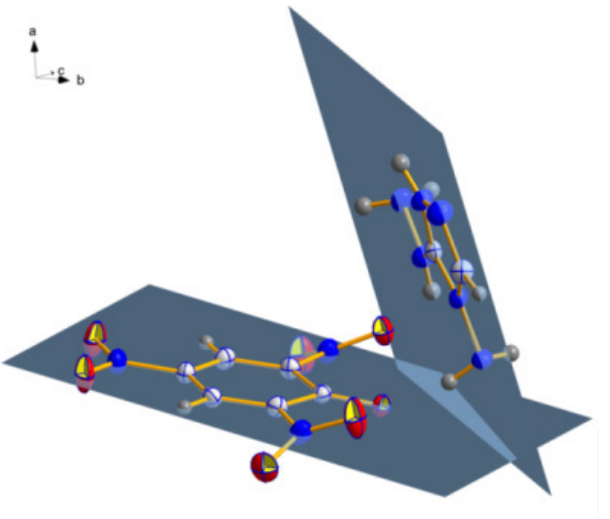


(a)

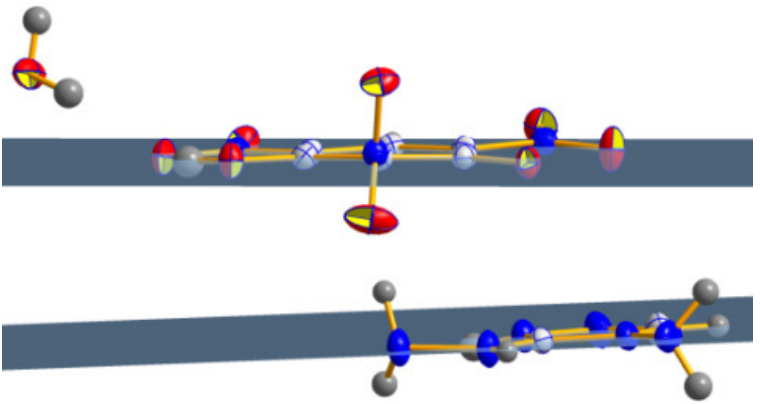

(b)

**Figure 2.** Plane view of (a) HATr·PA and (b) HATr·TNR·$H_2O$ in unit cell.

**Thermal decomposition**

In order to investigate the thermal behavior of the two salts, DSC and TG-DTG curves at a linear heating rate of 5 K·min$^{-1}$ were recorded in a nitrogen atmosphere (Figures 3 and 4).

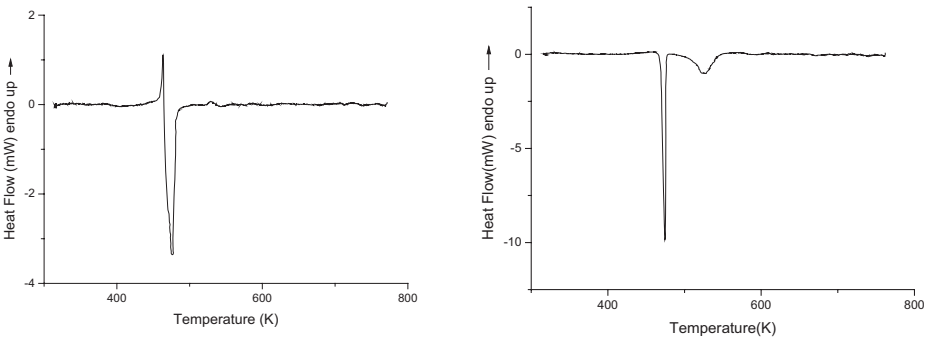


(a) (b)

**Figure 3.** DSC curves of (a) HATr·PA and (b) HATr·TNR·$H_2O$ at 5 K·min$^{-1}$.

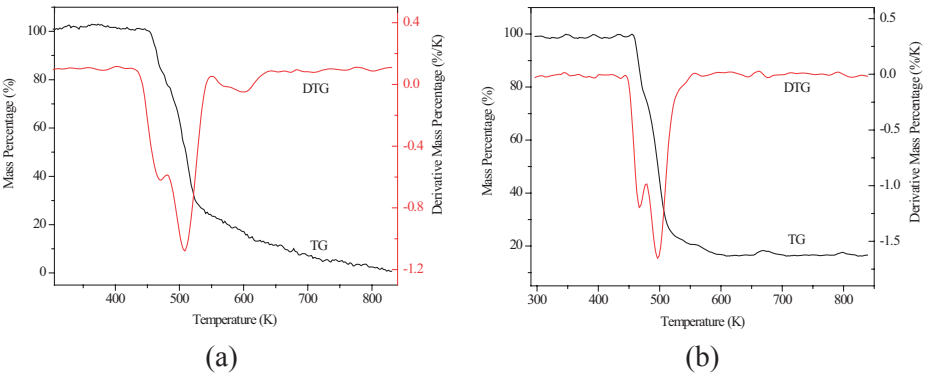


**Figure 4.** TG-DTG curves of (a) HATr·PA and (b) HATr·TNR·$H_2O$ at 5 K·$min^{-1}$.

For HATr·PA, the DSC curve shows two processes: one endotherm at 449.1 K, and one exotherm commencing at 464.6 K with a peak temperature of 476.2 K, whilst the TG-DTG curves indicate three stages in the process of thermal decomposition. The first mass loss (15.7%) occurs at 445.7 K. The second mass loss (53.3%) occurs at 523.2 K. The final stage is a slow process of thermal decomposition with continuous mass loss and no residue remaining.

For HATr·TNR·$H_2O$, the DSC curve shows that there are two decomposition processes: one sharp exotherm occurs at 461.8 K, with a further broad exotherm at 524.7 K (maximum). The TG-DTG curves also indicate two mass loss stages and one slow loss in the process of thermal decomposition. The first mass loss (22.4%) occurs at 457.6 K. The second mass loss (50.6%) occurs at 474.1 K. The final stage is a slow process of thermal decomposition with continuous mass loss and almost no residue remaining.

The heats of combustion and formation are significant characteristics for the assessment of the energetic properties of a new compound. The constant-volume heats of combustion ($Q_v$) of HATr·PA and HATr·TNR·$H_2O$ were -11.5237 MJ·$kg^{-1}$ and -10.2348 MJ·$kg^{-1}$, respectively, as measured by oxygen bomb calorimetry under $O_2$.

The bomb equations are as follows (Eqs. 1 and 2):

$$C_8H_9N_9O_7 + 27/4\ O_2 \rightarrow 8CO_2 + 9/2H_2O + 9/2N_2 \quad (1)$$

$$C_8H_{11}N_9O_9 + 25/4O_2 \rightarrow 8CO_2 + 11/2H_2O + 9/2N_2 \quad (2)$$

The energies of combustion are as follows (Eqs. 3 and 4) ($Q_p$: constant-pressure energy of combustion):

$$\Delta H[\text{HATr·PA}] = Q_P = Q_V + \Delta nRT = -3941.149\ \text{kJ·mol}^{-1} = -11.4822\ \text{MJ·kg}^{-1} \quad (3)$$

$$\Delta H[\text{HATr·TNR·H}_2\text{O}] = Q_P = Q_V + \Delta nRT = -3845.696\ \text{kJ·mol}^{-1} = -10.1938\ \text{MJ·kg}^{-1} \quad (4)$$

**Non-isothermal kinetic analyses**

Kissinger's method [9] and Ozawa-Doyle's method [10] are widely used to determine an apparent activation energy [11]. Using the first exothermic peak temperatures measured at four different heating rates (5, 10, 15, 20 $\text{K·min}^{-1}$), Kissinger's and Ozawa-Doyle's methods were applied to obtain the kinetic parameters for the two salts. The Kissinger (Eq. 5) and Ozawa (Eq. 6) equations are as follows, respectively:

$$\frac{d\ln(\beta/T_P^2)}{d(1/T_P)} = -\frac{E_a}{R} \quad (5)$$

$$\log\beta + \frac{0.4567E_a}{RT_P} = C \quad (6)$$

where: $T_p$ is the peak temperature, K; $R$ is the gas constant, 8.314 $\text{kJ·mol}^{-1}\text{·K}^{-1}$; $\beta$ is the linear heating rate, $\text{K·min}^{-1}$; $C$ is a constant.

From the original data, the apparent activation energies $E_k$ and $E_o$, the pre-exponential factor $A_k$ and the linear coefficients $R_k$ and $R_o$ were determined and are listed in Table 3 ($k$ and $o$ means Kissinger's method and Ozawa-Doyle's method, respectively).

**Table 3.** Peak temperatures of the first exothermic stage at different heating rates, and the kinetic parameters, for HATr·PA and HATr·TNR·$H_2O$

| $\beta$ [$\text{K·min}^{-1}$] | $T_P$ of HATr·PA | $T_P$ of HATr·TNR·$H_2O$ |
|---|---|---|
| 5 | 476.2 | 474.3 |
| 10 | 483.3 | 483.6 |
| 15 | 494.4 | 496.7 |
| 20 | 501.5 | 507.8 |
| Kissinger's method $E_k$ [$\text{kJ·mol}^{-1}$], ln $A_k$, $R_k$ | 95.145, 5.035, 0.9428 | 71.663, 4.181, 0.9358 |
| Ozawa-Doyle method $E_o$ [$\text{kJ·mol}^{-1}$], $R_o$ | 98.208, 0.9512 | 75.909, 0.9480 |

The calculated results using both methods correspond well with each other, and they are all in the normal range of kinetic parameters for the thermal decomposition of solid materials [12]. The apparent activation energy for

HATr·TNR·$H_2O$ is almost 23 kJ·mol$^{-1}$ lower than that for HATr·PA. This reveals that the energy barrier encountered for decomposition of HATr·TNR·$H_2O$ is smaller and thus this salt is more easily decomposed, which is in agreement with the DSC curves.

The Arrhenius equations for the two compounds can be expressed as follows:

$\ln k = 5.035 - 96.302\times10^3/(RT)$ for HATr·PA

$\ln k = 4.181 - 73.202\times10^3/(RT)$ for HATr·TNR·$H_2O$

**Calculation of the critical temperature for thermal explosion, $\Delta S^{\neq}$, $\Delta H^{\neq}$ and $\Delta G^{\neq}$**

Using Eq. (7) [13], the value of the peak temperature ($T_{p0}$), corresponding to $\beta\rightarrow0$, was obtained, where $a$, $b$ and $c$ are coefficients.

$$T_{pi} = T_{p0} + a\beta + b\beta^2 + c\beta^3 \tag{7}$$

The corresponding critical temperature of thermal explosion ($T_b$) is obtained using Eq. (8) [13], where $R$ is the gas constant, and $E$ is the value of $E_k$ by Kissinger's method.

$$T_b = \frac{E - \sqrt{E^2 - 4ERT_{p0}}}{2R} \tag{8}$$

The entropy of activation ($\Delta S^{\neq}$), the enthalpy of activation ($\Delta H^{\neq}$) and the free energy of activation ($\Delta G^{\neq}$) of the decomposition reaction corresponding to $T = T_{p0}$, $E_a = E_k$ and $A = A_k$ (obtained by Kissinger's method) were obtained using Eqs. (9), (10) and (11) [13].

$$A = \frac{k_B T}{h} e^{\Delta S^{\neq}/R} \tag{9}$$

$$\Delta H^{\neq} = E - RT \tag{10}$$

$$\Delta G^{\neq} = \Delta H^{\neq} - T\Delta S^{\neq} \tag{11}$$

where $k_B$ is the Boltzmann constant ($1.381\times10^{-23}$ J·K$^{-1}$·) and $h$ is Planck's constant ($6.626\times10^{-34}$ J·s). The calculated critical temperature of thermal explosion and the thermodynamic parameters are listed in Table 4.

**Table 4.** Calculated critical temperature of thermal explosion and thermodynamic parameters

| | $T_{P0}$ (K) | $T_b$ (K) | $\Delta H^{\neq}$ (kJ·mol$^{-1}$) | $\Delta G^{\neq}$ (kJ·mol$^{-1}$) | $\Delta S^{\neq}$ (J·K$^{-1}$·mol$^{-1}$) |
|---|---|---|---|---|---|
| HATr·PA | 481.1 | 484.9 | 93.41 | 135.05 | -200.06 |
| HATr·TNR·$H_2O$ | 474.6 | 479.3 | 69.98 | 111.69 | -206.89 |

The value of the critical temperature of thermal explosion for HATr·PA was a little higher than that for HATr·TNR·$H_2O$. The thermodynamic parameters followed the same pattern as with the thermal explosion, indicating that HATr·TNR·$H_2O$ has a greater tendency for the occurrence of an explosion.

**Sensitivity tests**

The impact and friction sensitivities, as well as the flame sensitivity, were determined according to Chinese Standards [14]. The results of these tests on HATr·PA and HATr·TNR·$H_2O$ are listed in Table 5.

**Table 5.** Results of sensitivity tests on HATr·PA and HATr·TNR·$H_2O$

| | HATr·PA | HATr·TNR·$H_2O$ |
|---|---|---|
| Friction sensitivity (%) | 60 | 0 |
| Impact sensitivity, $h_{50}$ (cm) | 31.45 | 0 |
| Flame sensitivity, $h_{50}$ (cm) | 12.41 | 18.24 |

The results showed that HATr·PA is more sensitive than HATr·TNR·$H_2O$ to the three kinds of stimulus.

## Conclusions

Two energetic salts HATr·PA and HATr·TNR·$H_2O$ were synthesized and characterized. Their crystal structures were determined at low temperature. Thermal analysis indicated that there was either no or one endothermic process and one or two exothermic processes, with no residue left at 850 K. The energies of combustion of HATr·PA and HATr·TNR·$H_2O$ are -11.4822 MJ·kg$^{-1}$ and -10.1938 MJ·kg$^{-1}$, respectively. Non-isothermal kinetic analysis indicated that the Arrhenius equation for HATr·PA and HATr·TNR·$H_2O$ can be expressed as follows:

$\ln k = 5.035 - 96.302\times10^3/(RT)$ (for HATr·PA)

$\ln k = 4.181 - 73.202\times10^3/(RT)$ (for HATr·TNR·$H_2O$)

Moreover, the values of the critical temperature for thermal explosion, $\Delta S^{\neq}$, $\Delta H^{\neq}$ and $\Delta G^{\neq}$ are 484.9 K, 93.41 kJ·mol$^{-1}$, 135.05 kJ·mol$^{-1}$, -200.06 J.K$^{-1}$·mol$^{-1}$ respectively for HATr·PA, and 479.3 K, 69.98 kJ·mol$^{-1}$ , 111.69 kJ·mol$^{-1}$, -206.89 J·K$^{-1}$·mol$^{-1}$, respectively for HATr·TNR·$H_2O$. The flame sensitivity measurements showed that the 50% flame heights were 12.41 cm and 18.24 cm for HATr·PA and HATr·TNR·$H_2O$, respectively. Above all, the results indicate that these two compounds have certain potential applications as gunpowder and propellant materials.

**Acknowledgements**

We gratefully acknowledge the Program for New Century Excellent Talents in University (No. NCET-09-0051), the project of State Key Laboratory of Science and Technology (No. QNKT11-06 and ZDKT12-03).

## References

[1] a) Drake G.W., Hawkins T.M., Boatz J., Hall L., Vij A., Experimental and Theoretical Study of 1,5-Diamino-4-H-1,2,3,4-tetrazolium Perchlorate, *Propellants Explos. Pyrotech.*, **2005**, *30*(2), 156-163; b) Drake G.W., Hawkins T.M., Brand A., Hall L., Mckay M., Energetic, Low-melting Salts of Simple Heterocycles, *Propellants Explos. Pyrotech.*, **2003**, *28*(4), 174-180; c) Xue H., Twamley B., Shreeve J.M., Energetic Azolium Azolate Salts, *Inorg. Chem.*, **2005**, *44*, 5068-5072; d) Gao H., Ye C.F., Twamley B., Shreeve J.M., Energetic Bicyclic Azolium Salts, *Chem. Eur. J.*, **2006**, *12*, 9010-9018.

[2] a) Smiglak M., Reichert W.M., Holbrey J.D., Wilkes J.S., *et al*., Combustible Ionic Liquids by Design: is Laboratory Safety Another Ionic Liquid Myth?, *Chem. Commun.*, **2006**, *24*, 2554-2556; b) Huang Y.G., Gao H.X., Twamley B., Shreeve J.M., Nitroamino Triazoles: Nitrogen-rich Precursors of Stable Energetic Salts, *Eur. J. Inorg. Chem.*, **2008**, *16*, 2560-2568; c) He L., Tao G.H., Parrish D.A., Shreeve J.M., Liquid Dinitromethanide Salts, *Inorg. Chem.*, **2010**, *50*, 679-685.

[3] a) Gao H., Ye C., Gutpa O.D., Xiao J.C., Hiskey M.A., 2,4,5-Trinitroimidazole-based Energetic Salts, *Chem. Eur. J.*, **2007**, *13*, 3853-3860; b) Fischer N., Klapötke T.M., Stierstorfer J., Explosives Based on Diaminourea, *Propellants Explos. Pyrotech.*, **2011**, *36*, 225-232; c) Fischer N., Klapötke T.M., Piercey D.G., Stierstorfer J., Hydroxylammonium 5-Nitriminotetrazolates, *Z. Anorg. Allg. Chem.*, **2012**, *638*(2), 302-310.

[4] a) Crawford M.J., Klapötke T.M., Martin F.A., Sabaté C.M., Energetic Salts of the Binary 5-Cyanotetrazolate Anion ($[C_2N_5]^-$) with Nitrogen-Rich Cations, *Chem. Eur. J.*, **2012**, *17*, 1683-1695; b) Klapötke T.M., Sabaté C.M., *Cent. Eur. J. Energ. Mater*., **2010**, *7*(2), 161-173; c) Fischer N., Klapötke T.M., Stierstorfer J., Less

Sensitive Transition Metal Salts of the 5-Nitrotetrazolate Anion, *Z. Anorg. Allg. Chem.*, **2011**, *637*, 1273-1276; d) Xue H., Twamley B., Shreeve J.M., Energetic Quaternary Salts Containing bi(1,2,4-triazoles), *Inorg. Chem.*, **2005**, *44*, 7009-7013.

[5] a) Xue H., Gao H., Twamley B., Shreeve J.M., Energetic Salts of 3-Nitro-1,2,4-triazole-5-one, 5-Nitroaminotetrazole, and other Nitro-substituted Azoles, *Chem. Mater.*, **2007**, *19*, 1731-1739; b) Schmidt M.W., Gordon M.S., Boatz J.A., Triazolium-based Energetic Ionic Liquids, *J. Phys. Chem. A*, **2005**, *109*, 7285-7295; c) Wang Q., Li J.Z., Yu H.J., Fu X.L., Fan X.Z., Ji P.Y., Review on Azotetrazolate Nonmetal Salts, *Chin. J. Energ. Mater.*, **2010**, *5*, 592-598; d) Singh R.P., Verma R.D., Meshri D.T., Shreeve J.M., Energetic Nitrogen-rich Salts and Ionic Liquids, *Angew. Chem. Int. Ed.*, **2006**, *45*, 3584-3601.

[6] Cardillo P., Dellavedova M., Gigante L., Lunghi A., Synthesis, Spectroscopic and Thermal Characterization of Azido-1,2,4-triazoles: A Class of Heteroarenes with a High Nitrogen Content, *Eur. J. Org. Chem.*, **2012**, *6*, 1195-1201.

[7] Sheldrick G.M., SHELXS-97, *Program for Crystal Structure Determination*; University of. Göttingen: Germany, **1997**.

[8] Sheldrick G.M., SHELXL-97, *Program for Crystal Structure Refinement*, University of Göttingen, Germany, **1997**.

[9] Kissinger H.E., Raction Kinetics in Differential Thermal Analysis, *Anal. Chem.*, **1957**, *18*, 1702-1706.

[10] Ozawa T.A., A New Method of Analyzing Thermo-gravimatric Data, *Bull. Chem. Soc. Jpn.*, **1965**, *38*, 1881-1886.

[11] Zhang Y.Q., Guo Y., Joo Y.H., Parrish D.A., Shreeve J.M., 3,4,5-Trinitropyrazole-Based Energetic Salts, *Chem. Eur. J.*, **2010**, *16*, 10778-10784.

[12] a) Li Z.M., Xie S.H., Zhang J.G., Feng J.L., Wang K., Two High Nitrogen Content Energetic Compounds: 3,6-Diguanidino-1,2,4,5-Tetrazine and Its Diperchlorate, *J. Chem. Eng. Data*, **2012**, *57*, 729-736; b) Wu B.D., Zhang J.G., Zhang T.L., Yang L., Zhou Z.N., Two Environmentally Friendly Energetic Compounds, $[Mn(AZT)_4(H_2O)_2](PA)_2 \cdot 4H_2O$ and $[Co(AZT)_2(H_2O)_4](PA)_2$, Based on 3-Azido-1,2,4-triazole (AZT) and Picrate (PA), *Eur. J. Inorg. Chem.*, **2012**, 1261-1268; c) Wu B.D., Wang S.W., Yang L., Zhang T.L., Zhang J.G., Preparation, Crystal Structures, Thermal Decomposition and Explosive Properties of Two Novel Energetic Compounds $M(IMI)_4(N_3)_2$ (M = Cu(II) and Ni(II), IMI = Imidazole): The New High-Nitrogen Materials (N > 46%), *Eur. J. Inorg. Chem.*, **2011**, 2616-2623.

[13] Diaz D.D., Punna S., Holzer P., Mcpherson A.K., Sharpless K.B., Fokin V.V., Finn M.G., Click Chemistry in Materials Synthesis. 1. Adhesive Polymers from Copper-catalyzed Azide-alkyne Cycloaddition, *J. Polym. Sci., Part A: Polym. Chem.*, **2004**, *42*, 4392-4403.

[14] Zhang T.L., Hu R.Z., Xie Y., *et al*., The Estimation of Critical-temperatures of Thermal-explosion for Energetic Materials using Nonistheramal DSC, *Thermochim. Acta*, **1994**, *244*, 171.

[15] Liu Z.T., Lao Y.L., *Initiation Explosive Experimental*, Beijing Institute of Technology, China, **1995**.